

# Spatio-Temporal Image Fusion using Landsat-8 and Himawari-8 Satellite Imagery

Hsuan-Chi Ho<sup>1</sup> Chih-Yuan Huang<sup>2</sup>

<sup>1</sup> Department of Civil Engineering, National Central University, Taiwan

Email: hsuanci@g.ncu.edu.tw

<sup>2</sup> Center for Space and Remote Sensing Research, National Central University, Taiwan

Email: cyhuang@csrsr.ncu.edu.tw

**KEY WORDS:** Image fusion, STARFM, Himawari-8, Landsat-8

**ABSTRACT:** Satellite remote sensing images provide periodical and multispectral information about the ground surface, which empowers various monitoring applications. Among the applications, some of them requires high spatial and temporal resolution, including disaster management, crop phenology monitoring, land cover change detection, etc. In order to provide high spatial and temporal information, image fusion techniques were proposed to integrate high-spatial-resolution satellite imagery with high-temporal-resolution imagery, such as the spatial and temporal adaptive reflectance fusion model (STARFM). Previous studies applied the STARFM method on Landsat and Moderate-resolution Imaging Spectroradiometer (MODIS) satellite images to provide high spatial and high temporal images. With the advance of satellite technology, a new satellite, Himawari-8, has a 10-minute temporal resolution, which is much higher than that of MODIS, and its spatial resolution is similar to MODIS. This research tries to fuse the Landsat-8 and Himawari-8 images to provide images with high spatial resolution and very high temporal resolution. On the preprocessing step, we use affine transformation for geometric correction. Then we use the STARFM method to fuse Landsat-8 images with Himawari-8 images to produce 30-meter-spatial-resolution and 10-minute-temporal-resolution images. Finally, in order to verify the result of this research, we apply the fused images to estimate aerosol optical depth (AOD) and compare with in-situ observations. Overall, this research uses Himawari-8 and Landsat-8 image to produce images with high spatial and temporal resolutions. The fused images could provide timely information to assist various monitoring applications.

## 1. Introduction

### 1.1 Background

With the advance of satellite technology, more satellites have been launched in recent years, and some of them provide high spatial resolution satellite images including Worldview-3 (30cm), Landsat-8 (15-30m), etc. Thus, many studies using with high spatial resolution satellite images for land cover monitoring, such as (Vogelmann et al., 2001). However, satellites with high spatial resolution usually have low temporal resolution. For example, the temporal resolution of Landsat is 16-day, which limits its use in continuous monitoring applications. On the other hand, satellites with high temporal resolution could be applied for time-critical applications, such as (Brakenridge et al., 2006) using Terra/Aqua Moderate-resolution Imaging Spectroradiometer (MODIS) satellite images for disaster management. MODIS provides high temporal resolution images (1-2 day), but provides coarse spatial resolution (250m to 1000m) observations. Hence, in order to provide high spatial and temporal information, image fusion techniques were proposed to integrate high-spatial-resolution satellite imagery with high-temporal-resolution imagery.

However, traditional methods focus on enhancing spatial resolution of multispectral images by combining panchromatic image with multispectral image, include pan-sharpening (Padwick et al., 2010). However, traditional methods mainly focus on enhancing the spatial resolution instead of enhancing spatial and temporal resolutions. Thus, some spatio-temporal image fusion methods were proposed.

Spatial and temporal image fusion methods try to integrate high-spatial-resolution satellite imagery with high-temporal-resolution imagery to provide high spatial and high temporal images. The key idea of spatial and temporal image fusion is to find the relationship between fine resolution image and coarse resolution image for predicting high spatial and high temporal satellite images, such as spatial and temporal adaptive reflectance fusion model (STARFM) (Gao et al., 2006).

The STARFM method applies Landsat and MODIS satellite images to generate high spatial and high temporal images every one to two days. However, with the advance of satellite technology, a new satellite, Himawari-8, has a 10-minute temporal resolution, which is much higher than that of MODIS, and wavelengths between Himawari-8 and Landsat-8 are similar. Thus, we have the opportunity to apply image fusion method to fuse the Landsat-8 and Himawari-8 to provide a high spatial resolution image every 10 minutes.

Table 1. Wavelengths of Himawari-8 and Landsat-8

Himawari-8		Landsat-8	
Band Number	Central wave length (nm)	Band Number	Central wave length (nm)
1	470.6	2	482.5
2	510	3	561.5
3	639.1	4	654.5
4	856.7	5	865
5	1610.1	6	1608.5
6	2256.8	7	2200.5

In general, this research tries to apply the STARFM method on the Landsat-8 and Himawari-8 images to provide high spatial (30m) and high temporal (10-minute) resolution images. Finally, in order to verify the result of this research, we apply the fused images to estimate aerosol optical depth (AOD) and compare with in-situ observations.

## 2. Methodology

Figure 1 shows the overall workflow of this research, including two stages. The input data contains the Landsat-8 and Himawari-8 images collected at  $T_k$  and a Himawari-8 image at  $T_0$ . And the main purpose is to generate a high spatial resolution image at  $T_0$  using the above images. The first stage is the preparation stage, which mainly contains the geometric correction of satellite images and the classification of the Landsat-8 image at  $T_k$ . The second stage performs the STARFM image fusion process to predict the high spatial resolution image at  $T_0$ .

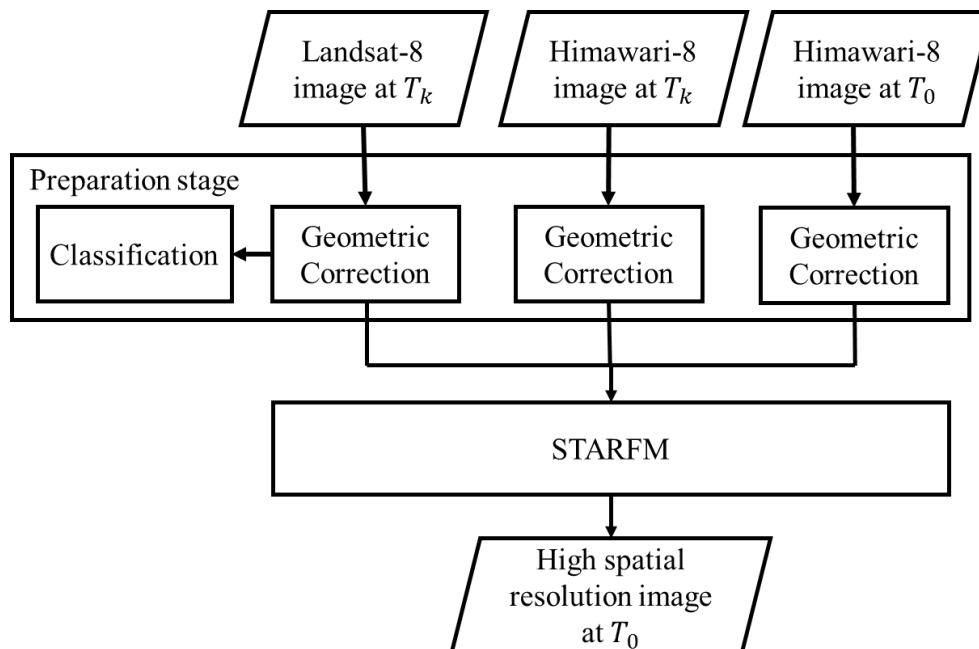


Figure 1. Workflow

## 2.1 Preparation stage

In order to integrate high-spatial-resolution satellite imagery with high-temporal-resolution imagery, those images should be first geographically registered with each other. This step is important for image fusion. If there is an offset between images, unnecessary information will be included in the image fusion process. In this research, we manually select the tie points in the images and then apply affine transformation for geometric correction.

In addition, this stage also performs image classification on the Landsat-8  $T_k$  image. The classification result is mainly for the STARFM image fusion method to select neighboring pixels. In this research, we applied the K-Means algorithm for the classification.

## 2.2 STARFM

The key idea of STARFM is to find the surface reflectance relationship between fine resolution and coarse resolution image at  $T_k$  as Equation. 1 (Gao et al, 2006) shows. And then STARFM applies the difference between fine resolution and coarse resolution image at  $T_k$  to predict high spatial and high temporal image at  $T_0$ .

$$L(x_i, y_j, t_k) = M(x_i, y_j, t_k) + \varepsilon_K \quad (1)$$

The  $\varepsilon_K$  means the difference between fine resolution and coarse resolution image at  $T_k$ . This difference could be caused by the bandwidth difference between images and solar geometry (Gao et al, 2006).

However, using single pixel to predict image would be easily affected by noises. Thus, the STARFM utilizes more information in the image fusion process by including neighboring pixels as shown in Equation. 2 (Gao et al, 2006).

$$L(x_{w/2}, y_{w/2}, t_k) = \sum_i^w \sum_j^w \sum_k^n W_{ijk} \times (M(x_i, y_j, t_0) + \varepsilon_k) \quad (2)$$

In the  $x_{w/2}$ ,  $w$  is the size of search window. The  $W_{ijk}$  is the weight, which considers the spectrum, temporal, distance differences between the central pixel and neighboring pixels. Finally, we can use this equation to predict high spatial and high temporal images.

## 3. Preliminary result

In order to verify the result of this research, we apply the fused images to estimate aerosol optical depth (AOD) and compare with in-situ data observed by ground stations. In order to extract AOD from satellite images, we chose the dispersion coefficient method (Sifakis et al., 1992). The dispersion coefficient method can retrieve the AOD of satellite image by analyzing the relationship between AOD and image surface reflectance. The reference AOD is observed from ground station that should be cloud-free. The retrieval results are compared with the reference in-situ AOD data.

### 3.1 Satellite image fusion using Landsat-8 and Himawari-8 images

The details of testing dataset are shown in Table 2. The study area is at Zhongli, Taiwan. We have tested the proposed solution on 31 Himawari-8 images. The reference Landsat-8 and Himawari-8 images are collected at 10:20. Figure 2 shows a part of the experimental result, includes the images used in STARFM and the predicted images at 11:00, 12:00, 13:00, and 14:00. In general, the STARFM can successfully produce high spatial resolution images every 10 minutes.

Table 2. Dataset

Study area	Zhongli, Taiwan
Source of reference AOD	AERONET (Aerosol Robotic NETWORK)
Source of satellite image	Landsat-8 from USGS on 11/16 at 10:20, and Himawari-8 from central weather bureau of Taiwan on 11/16 at 8:20, 8:30, 8:50, 9:00, 9:10, 9:20, 9:30, 9:40, 9:50, 10:00, 10:10, 10:20, 10:30, 11:00, 11:10, 11:20, 11:30, 11:40, 11:50, 12:00, 12:10, 12:20, 12:30, 12:40, 12:50, 13:00, 13:10, 13:20, 13:30, 13:40, 13:50, 14:00.

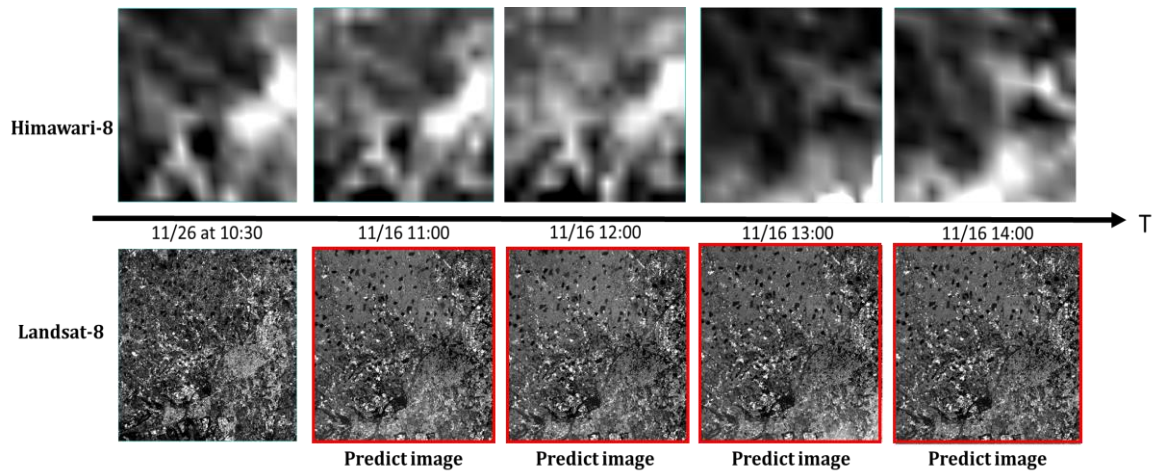


Figure 2. Image fusion results

### 3.2 Validation of predicted images

We use the dispersion coefficient to retrieve AOD from Himawari-8. The result is shown in Figure 3. In addition, we compute RMSE of AOD by comparing the retrieved AOD with reference AOD from the ground station, as shown in Table 3. We can observe that the AOD of Himawari-8 calculated with  $9 \times 9$  window size has the smallest RMSE. However, we have overestimated AOD of Himawari-8 at 8:20. The main reason of that is the radiance is lower than the reference image at 10:20.

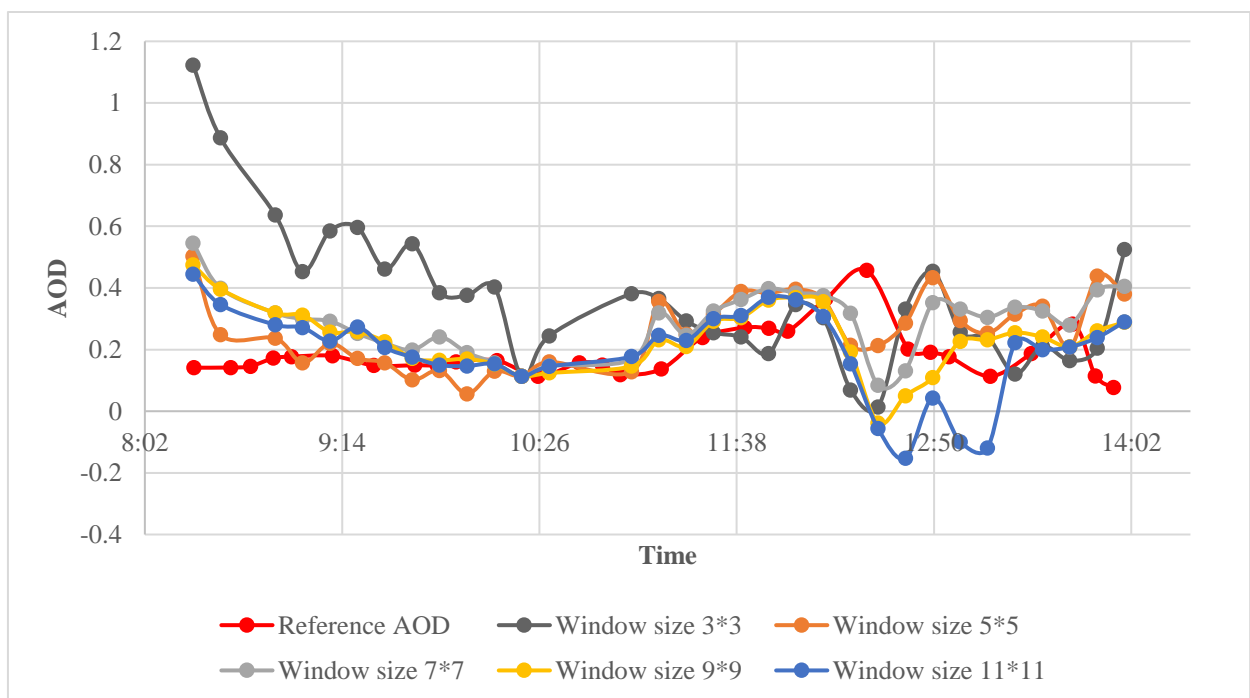


Figure 3. AOD from original Himawari-8 images

We use the dispersion coefficient to retrieve AOD of predicted images, as shown in Figure 4. We can find that the AOD retrieved with  $15 \times 15$  window size has the smallest RMSE. However, most of the AOD of predicted images underestimated the AOD, especially at the early morning and late afternoon. We believe the reason is because of the radiance of those predicted images are lower than the AOD reference image at 10:20.

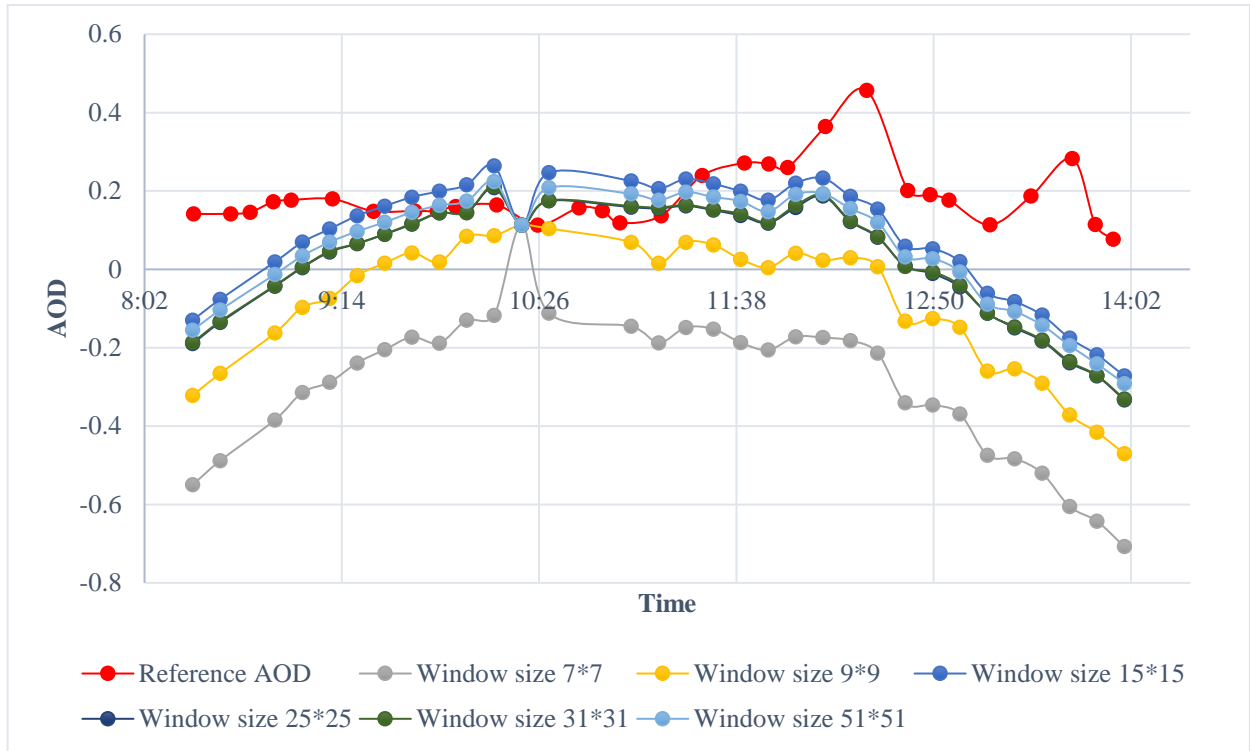


Figure 4. AOD from predicted images

Table 3. RMSE of AOD

Window size of AOD retrieval	RMSE of Himawari-8	Window size of AOD retrieval	RMSE of Predict
3*3	0.383	7*7	0.549
5*5	0.162	9*9	0.346
7*7	0.173	15*15	0.192
9*9	0.135	25*25	0.234
11*11	0.158	31*31	0.232
		51*51	0.210

#### 4. Conclusions and future work

This research aims at applying the STARFM image fusion method on Landsat-8 and Himawari-8 satellite images in order to produce high spatial and temporal resolution images. While Himawari-8 generates images every 10 minutes, the fused images have very high temporal resolution, which could be used in various time-critical applications. In this research, we validate the fused images by calculating the AOD from images and comparing with in-situ reference observations. Based on our experimental result, we can see that the STARFM algorithm can successfully produce high spatial and temporal resolution images. However, the retrieval of AOD still suffering from the problem of radiance differences between predicted images and the reference image. Therefore, in order to better compare with reference AOD observations, one of our future directions is to adjust the image radiance before calculating the AOD by using the predicted images. In addition, we will test our proposed solution by using more testing datasets.

## 5. Reference

Gao, F., Masek, J., Schwaller, M., & Hall, F. (2006). On the blending of the Landsat and MODIS surface reflectance: Predicting daily Landsat surface reflectance. *IEEE Transactions on Geoscience and Remote sensing*, 44(8), 2207-2218.

Padwick, C., Deskevich, M. I. C. H. A. E. L., Pacifici, F., & Smallwood, S. (2010, April). WorldView-2 pan-sharpening. In *Proceedings of the ASPRS 2010 Annual Conference*, San Diego, CA, USA (Vol. 2630).

Vogelmann, J. E., Howard, S. M., Yang, L., Larson, C. R., Wylie, B. K., & Van Driel, N. (2001). Completion of the 1990s National Land Cover Data Set for the conterminous United States from Landsat Thematic Mapper data and ancillary data sources. *Photogrammetric Engineering and Remote Sensing*, 67(6), pp. 650–662.

Brakenridge, R., & Anderson, E. (2006). MODIS-based flood detection, mapping and measurement: The potential for operational hydrological applications. In *Transboundary floods: reducing risks through flood management* (pp. 1-12).

Sifakis, N., & Deschamps, P. Y. (1992). Mapping of air pollution using SPOT satellite data. *Photogrammetric Engineering and Remote Sensing*, 58, 1433-1433.